Chemical Geology, 69 (1988) 111–126
Elsevier Science Publishers B.V., Amsterdam — Printed in The Netherlands

[3]

REDISTRIBUTION OF RARE-EARTH ELEMENTS DURING DIAGENESIS OF CARBONATE ROCKS FROM THE MID-PROTEROZOIC NEWLAND FORMATION, MONTANA, U.S.A.

JÜRGEN SCHIEBER*

Department of Geology, University of Oregon, Eugene, OR 97403 (U.S.A.)

(Received November 25, 1987; accepted for publication January 19, 1988)

Abstract

Schieber, J., 1988. Redistribution of rare-earth elements during diagenesis of carbonate rocks from the Mid-Proterozoic Newland Formation, Montana, U.S.A. Chem Geol., 69: 111–126.

REE data for carbonate rocks from the Mid-Proterozoic Newland Formation, Belt Supergroup, show variable degrees of relative REE enrichment when normalized to a composite shale of the Newland Formation. Most conspicuous are relative enrichments in LREE's and positive Eu anomalies. Possible coprecipitation of REE's in carbonates from seawater is much too small to account for the REE enrichment, thus only diagenetic REE enrichment has to be considered. By far the strongest LREE enrichment is observed in carbonates with interbedded shales. During diagenesis REE apparently moved from the shale partings to the adjacent limestone beds. Massive limestone units have considerably smaller REE enrichments (except in proximity to shales), suggesting that REE addition from formation waters is less efficient for supplying REE's than is local redistribution between shale and limestone beds. Early precipitation of diagenetic silica in pore spaces reduces REE enrichment in limestone beds by reducing their permeability. Dolostones are cemented by pervasive early-diagenetic silica and lack significant REE enrichment except for Eu, probably because silica cement prohibited access of REE-bearing pore waters. Positive Eu anomalies indicate reduction of Eu to the divalent state during diagenesis and relatively large mobility of divalent Eu.

1. Introduction

Concentrations of rare-earth elements (REE's) found in carbonate rocks are typically small when compared to those of terrigenous sendiments, but with relative proportions similar to those of average terrigenous sediments (Balashov et al., 1964; Haskin et al., 1968; Ronov et al., 1974; Jarvis et al., 1975). Parekh et al. (1977) constructed regression plots of REE vs. insoluble residue for a suite of carbonate rocks and showed that significant amounts of REE's are present in the carbonate phase of these rocks. Haskin et al. (1966) and McLennan et al. (1979) also concluded that the carbonate phase may carry considerable portions of the REE content of carbonate rocks. REE incorporation into carbonate minerals and the behaviour of REE's during diagenesis were investigated by Parekh et al. (1977), Scherer

**Present address*: Department of Geology, The University of Texas at Arlington, TX 76019, U.S.A.

0009-2541/88/$03.50

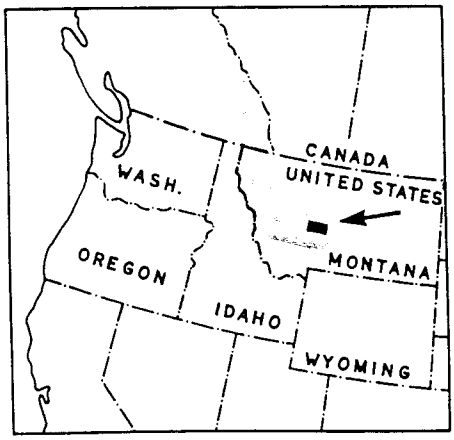

Fig. 1. Location and outline of Belt basin. Study area pointed out by *arrow*.

and Seitz (1980), and Shaw and Wasserburg (1985).

REE's in a large number of shales and carbonate samples from the Mid-Proterozoic Newland Formation, Montana, U.S.A., were determined as part of a study of Proterozoic sediments (Schieber, 1985). Samples from five different carbonate lithofacies types were examined.

2. Geology

The Newland Formation is part of the Belt Supergroup (Harrison, 1972) and occurs in an eastern extension of the Belt basin, the Helena embayment. An overview of the geology of the study area is given in Schieber (1986). Samples for this study were collected in the Little Belt Mountains (Fig. 1).

The Newland Formation has been subdivided into a lower and upper member by Nelson (1972), with the lower member consisting of a uniform sequence of dolomitic shales and the upper member consisting of intercalated packages of shales and carbonates. Carbonate units are between 10 and 70 m thick, and shale units are between 50 and 110 m thick (Schieber, 1985). All the samples analyzed for this study were collected from the upper member of the Newland Formation.

3. Analytical procedures

REE's were determined by instrumental neutron activation analysis (INAA), following the technique of Gordon et al. (1968). The samples were irradiated together with the U.S.G.S. standard rocks W-*1*, AGV-*1*, GSP-*1* and BCR-*1*, and with internal laboratory standards. Other elemental abundances that are reported in this study (SiO_2, Al_2O_3) were determined by X-ray fluorescence (XRF).

Precision and accuracy of the analytical data can be evaluated from the data for replicate analysis of standard rocks that are presented in Table I. These data suggest a precision better than $\pm 7\%$ for La, Ce, Sm and Eu, and of $\pm 10\%$ or better for Tb, Yb and Lu. In most samples a straight line could be drawn through the zone defined by error bars of Tb, Yb and Lu. Thus variations among heavier REE (HREE), if any, are obscured by analytical errors.

In order to examine REE distribution between carbonate minerals and terrigeneous fraction, leaching experiments were carried out on four limestone samples. Very dilute (0.3 *N*) cold HCl was used to dissolve the carbonate minerals and minimize leaching of other minerals. The acid treatment was carried out after irradiation in order to avoid any contamination by REE's during the separation process (only radioactive REE's, present before separation, will be registered). The soluble and residue fractions of each sample were separated by filtration. Liquid portions and filter papers were filled into separate plastic vials and then analyzed individually for REE's (Table II). The liquid specimens have a somewhat different geometric relationship to the analyzer crystal than the solid specimens (rolled up filter paper in vial), and this difference causes errors in the determination of absolute REE abundances. However, element ratios within a specimen do not suffer from this geometry effect because all elements are affected equally. The results of whole-rock REE determinations for these samples are also shown in Table II. It should be

TABLE I

Rare earth abundances (in ppm) in standard rocks (recommended values from Govindaraju, 1984)

Standard rock		La	Ce	Sm	Eu	Tb	Yb	Lu
AGV-*1*	(a)	36.9	71.9	6.0	1.67	0.9	1.88	0.27
	(b)	±0.32	±3.2	±0.13	±0.05	±0.07	±0.19	±0.015
	(c)	37.0	71.0	5.9	1.7	0.7	1.9	0.28
BCR-*1*	(a)	23.5	56.0	6.75	1.99	0.77	3.54	0.55
	(b)	±0.6	±3.8	±0.15	±0.05	±0.09	±0.16	±0.03
	(c)	25.0	53.9	6.6	1.96	1.0	3.4	0.55
GSP-*1*	(a)	175.0	449.0	25.4	2.4	1.45	2.1	0.257
	(b)	±3.1	±26.0	±0.26	±0.03	±0.14	±0.7	±0.006
	(c)	185.0	400.0	25.0	2.4	1.4	1.9	0.22
W-*1*	(a)	10.0	24.7	3.27	1.09	0.69	2.28	0.32
	(b)	±0.14	±1.7	±0.02	±0.03	±0.07	±0.15	±0.02
	(c)	10.0	23.0	3.5	1.11	0.65	2.1	0.34

(a) this study, 10 analyses of AGV-*1*, 9 analyses of BCR-*1*, 3 analyses of GSP-*1*; 5 analyses of W-*1*, (b) precision, ±1 standard deviation; (c) recommended values.

TABLE II

REE data for carbonate–residue pairs

Sample No.	La	La*	Ce	Ce*	Sm	Sm*	Eu	Eu*	Tb	Tb*	Yb	Yb*	Lu	Lu*	Whole-rock fraction
*20*C	21.8	14.4	37.4	24.7	3.7	2.44	0.73	0.48	0.41	0.27	0.82	0.54	0.14	0.09	0.66
*20*R	2.7	0.92	7.8	2.65	1.05	0.36	0.23	0.08	0.13	0.04	1.04	0.35	0.19	0.06	0.34
CWRAB		15.3		27.4		2.8		0.56		0.31		0.89		0.15	
MWRAB		15.3		27.7		3.1		0.58		0.26		0.92		0.16	
*23*C	9.8	7.06	18.2	13.1	1.43	1.03	0.52	0.37	0.18	0.13	0.37	0.27	0.066	0.05	0.72
*23*R	1.9	0.53	6.1	1.71	0.53	0.15	0.24	0.07	0.10	0.03	0.56	0.16	0.085	0.025	0.28
CWRAB		7.59		14.8		1.18		0.44		0.16		0.43		0.075	
MWRAB		9.06		15.5		1.53		0.53		0.12		0.37		0.06	
*33*C	16.6	14.3	25.4	21.8	2.90	2.5	0.51	0.44	0.23	0.2	0.70	0.6	0.08	0.07	0.86
*33*R	4.6	0.6	9.8	1.37	0.74	0.1	0.20	0.03	0.08	0.01	0.53	0.07	0.08	0.01	0.14
CWRAB		14.9		23.2		2.6		0.47		0.21		0.67		0.08	
MWRAB		14.0		24.8		2.3		0.49		0.21		0.66		0.09	
*39*C	20.5	12.3	35.6	21.4	4.04	2.4	0.67	0.4	0.42	0.25	1.05	0.63	0.11	0.07	0.6
*39*R	5.14	2.06	11.0	4.4	0.84	0.34	0.18	0.07	0.07	0.03	1.03	0.41	0.19	0.08	0.4
CWRAB		14.4		25.8		2.74		0.47		0.28		1.04		0.15	
MWRAB		13.5		29.1		2.6		0.5		0.33		0.9		0.14	

C and R after sample number indicates data are from carbonate and residue fraction, respectively; CWRAB = calculated whole-rock abundance (sum of REE contribution of carbonate and residue fraction to whole-rock abundance); MWRAB = measured whole-rock abundance (determined on rock powders, data from Table III).

*REE contribution of carbonate and residue fraction to whole-rock REE abundance calculated as the product of REE concentration and whole-rock weight fraction).

pointed out that because of above noted geometry effect, the actual REE ratios between liquid fraction and residue are probably slightly different from the ones shown in Table II. Only data for La, Ce, Sm, Eu, Tb, Yb and Lu are reported in this study, because other REE's could not be determined with satisfactory precision.

4. Normalization with the "Upper Newland Average Shale"

REE concentrations in sediments are commonly normalized to the North American Shale Composite or NASC (Haskin et al., 1968). In this study, however, a different approach was taken. Because REE distributions in carbonate rocks tend to follow closely the distribution of REE's in the terrigenous component of these rocks (Haskin et al., 1966; McLennan et al., 1979), normalization of REE concentrations in carbonate rocks to REE concentrations of directly associated terrigenous rocks should lead to a flat REE pattern. Any significant deviation of the REE distribution in the carbonate rocks from that of the terrigenous rocks should be easily detectable. However, if REE's in carbonate rocks are normalized to NASC, any discrepancy in REE distribution between NASC and the terrigenous rocks that are associated with these carbonate rocks will lead to "normalization anomalies" that complicate interpretation of REE patterns. In this study shales and carbonates from the Newland Formation were analyzed side by side, with the same procedure and the same equipment, and normalized to the same standard rock samples. Therefore, normalizing Newland carbonates to their associated shales will tend to minimize the impact of any hidden systematic analytical errors (caused by peculiarities of the analytical set-up) on the normalized REE patterns. In addition, this kind of normalization would allow one to "see through" REE variations in carbonates that are actually due to the terrigenous component.

Shales of the upper member of the Newland Formation are uniform in composition and show negative Eu anomalies when compared to NASC (Schieber, 1986). Petrographic studies show that the shales consist essentially of illite, quartz, dolomite, minor amounts of mica flakes (muscovite, ±biotite), detrital feldspar (mainly K-feldspar), and trace amounts of heavy minerals (tourmaline, zircon). Illite is by far the dominant aluminosilicate (>95%) in these shales, and positive correlation between La and Al_2O_3 (Schieber, 1986) shows that the REE's reside almost entirely in the illite. The composition of an average upper Newland shale was compiled from 32 individual analyses (data from Schieber, 1985, 1986). REE contents of the shale samples were weighted to take into account stratigraphic thickness of a sampled shale horizon and variations of sampling density. The REE content of the "Upper Newland Average Shale" (designated as UNAS in the remainder of the paper) is given in Table III.

5. Facies and REE patterns

Analytical results for 44 carbonate samples and 2 samples of calcareous shale are given in Table III. In the following paragraphs the REE patterns of each carbonate facies type are presented, together with a brief facies description and observations that pertain to diagenesis. Proximity to the shoreline and magnitude of terrigenous input determine the distribution of these lithofacies types within the basin, with facies C*1* and C*2* being deposited in a nearshore setting, and facies C*6* being deposited farthest offshore (Schieber, 1985).

Facies C1 consists of fine crystalline (5–10 μm crystal size) dolostone beds (5–100 cm thick). Carbonate packages as much as 5 m thick alternate with shale packages (some metres to 10 m thick). Dolomite crystals are embedded in a matrix of clay minerals and authigenic silica (Figs. 2 and 3). The small crystal size of the dolomite indicates a penecontemporaneous or very early diagenetic origin (Bathurst, 1983), UNAS-normalized REE patterns of facies C*1* are characterized by

TABLE III

Analyses of Newland carbonates (REE in ppm, other elements in %)

Sample No.	Al_2O_3 (%)	SiO_2 (%)	La	Ce	Sm	Eu	⊿Eu	Tb	Yb	Lu
1	4.05	29.0	11.6	24.2	2.75	0.52	0.15	0.23	0.93	0.21
2	5.52	42.7	13.2	29.0	2.77	0.55	0.12	0.34	1.2	0.2
3	4.11	34.8	11.2	24.0	2.36	0.62	0.27	0.27	0.89	0.13
4	4.0	33.2	12.2	27.7	2.28	0.59	0.24	0.29	0.8	0.13
5	1.32	11.7	7.47	13.1	1.2	0.22	0.04	0.13	0.43	0.08
6	0.5	15.3	4.5	8.5	0.83	0.14	0.01	0.1	n.d.	0.05
7	1.0	7.3	2.8	5.8	0.53	0.12	0.03	0.08	0.24	0.05
8	0.77	6.8	2.7	6.0	0.61	0.14	0.04	0.09	0.3	0.05
9	0.74	10.2	3.96	8.9	0.77	0.18	0.06	0.11	0.3	0.04
10	0.53	8.5	2.67	5.0	0.53	0.11	0.04	0.05	0.17	0.03
11	2.4	21.3	10.3	22.1	2.03	0.3	(*)	0.27	0.9	0.13
12	1.97	16.9	9.36	20.0	1.69	0.28	(*)	0.24	0.73	0.11
13	0.35	13.8	2.09	4.2	0.39	0.06	(*)	0.05	0.2	0.03
14	2.97	37.3	14.1	28.9	2.46	0.42	0.06	0.27	0.74	n.d.
15	1.07	6.3	11.8	20.5	1.59	0.34	0.09	0.2	0.51	0.09
16	0.99	6.2	6.27	9.2	1.06	0.21	0.06	0.11	0.25	0.06
17	0.32	1.9	3.53	4.2	0.44	0.08	0.01	0.055	0.17	0.03
18	0.53	3.8	1.77	3.2	0.3	0.08	0.04	0.033	n.d.	0.02
19	0.6	5.9	3.58	5.7	0.71	0.11	0.02	0.057	0.13	n.d.
20	3.56	21.0	15.3	27.7	3.1	0.58	0.16	0.26	0.92	0.16
21	1.84	15.5	19.8	37.2	3.0	0.54	0.10	0.33	0.99	0.13
22	1.43	22.8	7.3	15.0	1.13	0.27	0.09	0.15	1.13	0.27
23	1.42	31.1	9.06	15.5	1.53	0.53	0.32	0.12	0.37	0.06
24	0.76	5.4	5.4	8.96	0.66	0.17	0.07	0.09	0.21	0.036
25	0.4	4.8	2.88	5.76	0.48	0.1	0.03	0.055	0.17	n.d.
26	0.41	18.8	2.49	4.85	0.44	0.09	0.03	0.045	0.15	0.023
27	3.15	27.7	23.6	50.2	3.6	0.7	0.12	0.5	1.47	0.22
28	1.49	18.4	37.9	65.6	4.7	0.77	0.07	0.52	1.35	0.18
29	2.11	14.9	24.5	45.8	3.9	0.77	0.19	0.42	1.02	0.18
30	1.77	8.6	22.7	42.5	3.07	0.58	0.11	0.36	1.13	0.17
31	2.61	16.6	16.8	32.7	2.6	0.56	0.16	0.32	0.9	0.15
32	0.79	6.64	13.7	21.5	2.0	0.45	0.16	0.2	0.61	0.1
33	0.8	9.8	14.0	24.8	2.3	0.49	0.17	0.21	0.66	0.09
34	4.98	29.6	23.2	52.0	3.7	0.74	0.16	0.48	1.67	0.26
35	5.27	40.4	24.9	52.8	4.26	0.72	0.03	0.57	1.5	0.25
36	3.99	25.8	13.5	31.2	2.98	0.5	0.06	0.33	1.2	0.2
37	3.91	29.8	13.7	27.6	2.64	0.58	0.21	0.24	0.88	0.15
38	2.67	31.8	12.0	26.7	2.8	0.5	0.10	0.28	0.8	0.145
39	3.16	32.4	13.5	29.1	2.6	0.5	0.10	0.33	0.9	0.14
40	1.84	22.3	8.9	18.7	1.47	0.29	0.06	0.19	0.5	0.09
41	1.14	21.4	6.68	14.9	1.18	0.23	0.04	0.16	0.45	0.07
42	3.76	28.2	26.8	54.1	4.4	0.63	(*)	0.46	1.7	0.28
43	4.21	35.0	21.1	45.3	3.7	0.57	(*)	0.45	1.36	0.21
44	3.88	28.2	16.5	38.7	3.3	0.46	(*)	0.39	1.4	0.2
45	8.94	67.2	15.6	32.1	2.4	0.34	(*)	0.3	1.5	0.29
46	6.55	42.9	24.8	52.2	4.3	0.68	(*)	0.53	2.0	0.31
UNAS	-	-	26.0	54.1	4.42	0.69	-	0.57	2.21	0.39

n.d. = abundance not determined because of poor peak resolution; - = not present.
*No ⊿Eu calculated because of lack of positive Eu anomaly.

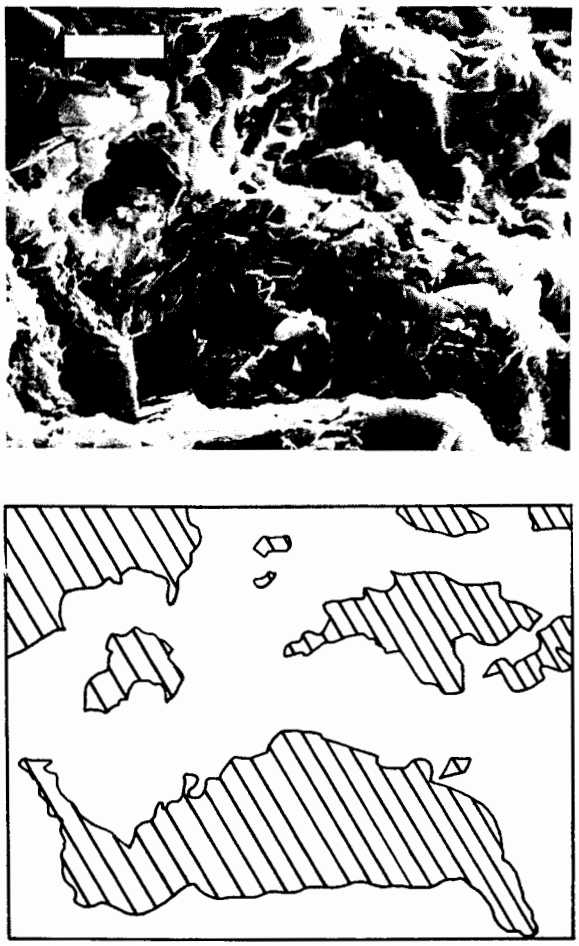

Fig. 2. Scanning electron microscopy photo of facies C1 dolostone. Dolomite areas (*dark grey*, lined in tracing below photo) surrounded by the silica-clay matrix (*light colour*, hackly surface). *Scale bar* is 5 μm long.

an essentially flat baseline (a line through La and Lu) and a distinct positive Eu anomaly (Fig. 4A).

Facies C2 is characterized by dolostone beds (1–15 cm thick) with irregularly shaped chert nodules (up to 10 cm across). Dolomite crystals do not exceed 25–30 μm in size, and are embedded in a sponge-like matrix of diagenetic silica (Fig. 5). The amount of matrix silica is variable and ranges from 6.8% to 21.3% in the analyzed samples. Cross-cutting relationships to other diagenetic features (Schieber, 1985) indicate that interstitial silica deposition occurred quite early in diagenesis. Facies C2 exhibits two types of REE patterns, one type that is essentially flat, and one type with a flat baseline and a positive Eu anomaly (Fig. 4B).

Facies C3 consists of limestone beds (3–25 cm thick) that are separated by beds of calcareous shale (1–30 cm thick). The carbonate beds are of concretionary origin and grew in a calcareous mud during early diagenesis (Fig. 6). Limestone beds consist mainly of interlocking calcite crystals with irregular outlines (10–100 μm in size) and small amounts of clay and quartz silt. Diagenetic silica is present between calcite crystals (Fig. 7), but is generally less prominent than in facies C1 and C2. Three types of REE patterns can be distinguished in facies C3, the first type (bottom of Fig. 4C) consists of essentially flat patterns without positive Eu anomalies. The second pattern type (middle of Fig. 4C) has a gently inclined baseline and a positive Eu anomaly. The third pattern type (top of Fig. 4C) has a relatively strongly inclined baseline and positive Eu anomalies.

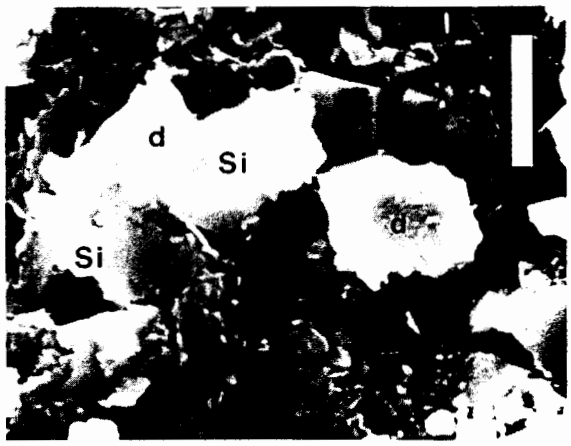

Fig. 3. Scanning electron microscopy photo of facies C1 dolostone. Two prominent dolomite rhombohedrons are marked by *d*. *Light areas* between the rhombohedrons (marked *Si*) consist of diagenetic silica. The area below the centre of the photo consists of clay minerals cemented by silica. The upper right-hand corner of the photo (to the left of the *scale bar*) shows dolomite crystals and dolomite molds in the silica-clay matrix. *Scale bar* is 5 μm long.

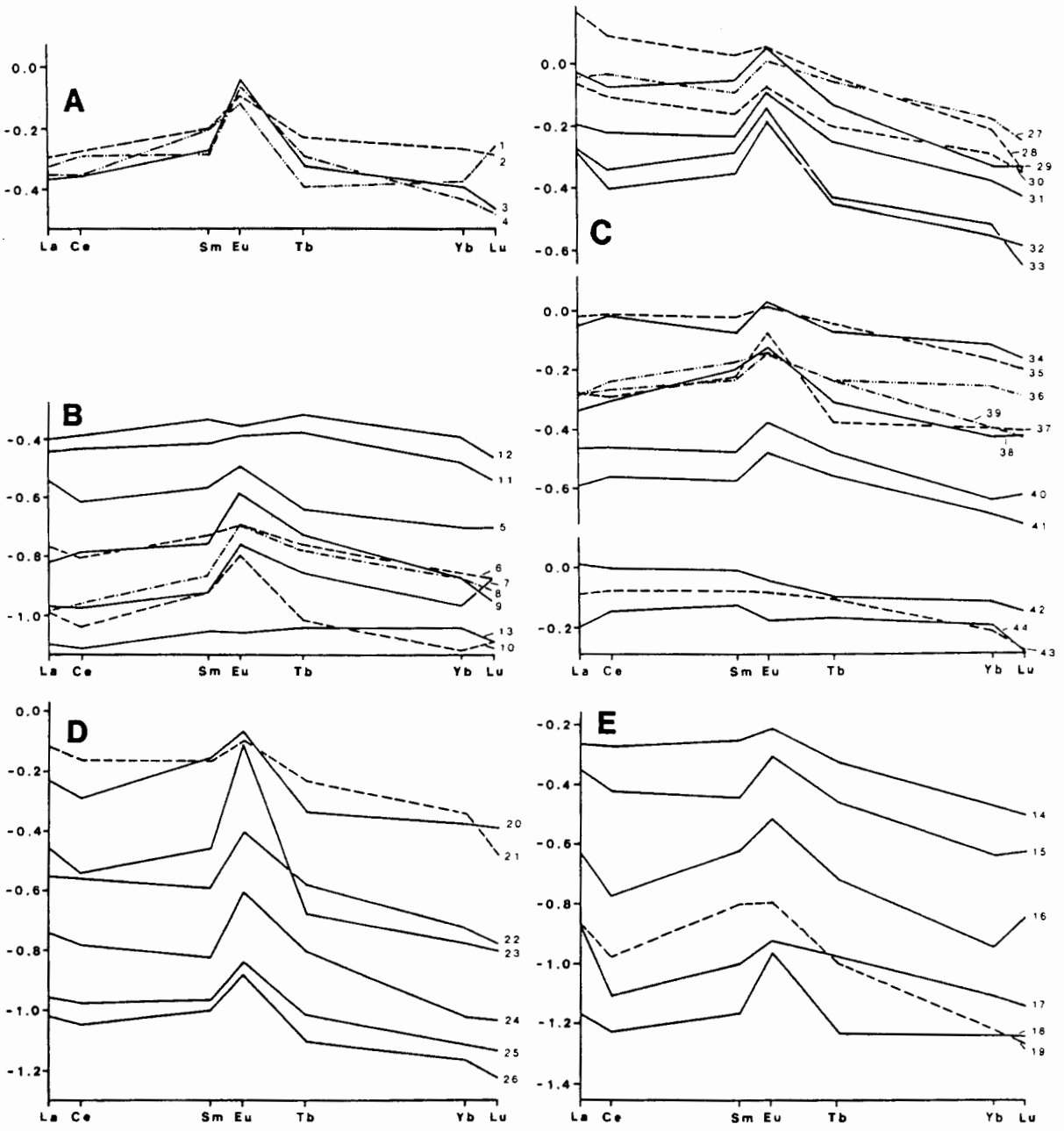

Fig. 4. Carbonate rock REE patterns of the various carbonate facies types in the Newland Formation: (A) patterns for facies C*1*; (B) patterns for facies C2; (C) = patterns for facies C*3*; (D) = patterns for facies C*4*; and (E) = patterns for facies C*6*. *Vertical axis* is the logarithm of the concentration ratio between sample and UNAS, *horizontal axis* is REE's by atomic number. The *numbers* to the right of REE patterns are the sample numbers from Table III.

Facies C4 consists of even bedded limestone (3–25 cm thick beds) with irregular interlocking calcite crystals (10–40 μm in size) and minor amounts of clay and quartz silt. Local concentrations of diagenetic silica are indicated by small chert nodules. No spongy silica frameworks (such as in facies C2) were observed. The REE patterns of this facies have

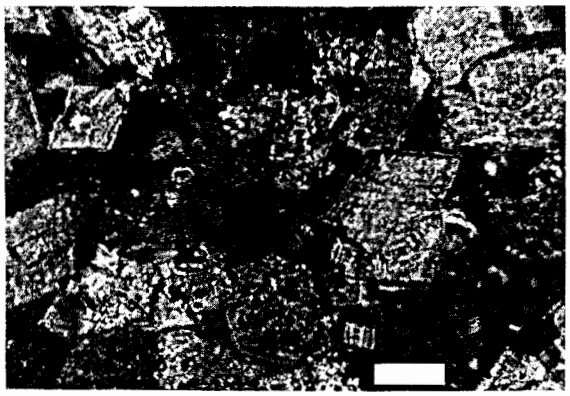

Fig. 5. Photomicrograph of facies C2 dolostone (crossed polarizers). *Dark mottled* spaces between dolomite crystals (rhombs) are filled with diagenetic silica cement. *Scale bar* is 20 μm long.

inclined baselines and positive Eu anomalies (Fig. 4D).

Facies C6 consists of bedded limestone (3–25 cm thick beds) that is characterized by sets of millimetre-scale laminations (a few cm to 20 cm thick). C6 is the purest limestone facies and consists predominantly of interlocking calcite crystals (5–40 μm in size) and minor amounts of clay and quartz silt. No chert nodules were found in this facies and diagenetic silica is of minor importance. The REE patterns of this

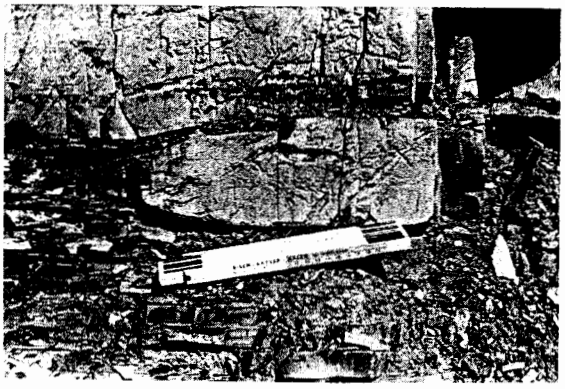

Fig. 6. Nodular limestone in facies C3. Note differential compaction around nodule. Laminations in shale are continuous into carbonate nodules and fan out when they enter the nodule (left edge of nodule), an indication of early-diagenetic (pre-compaction) nodule formation. The *ruler* has cm divisions and is 22 cm long.

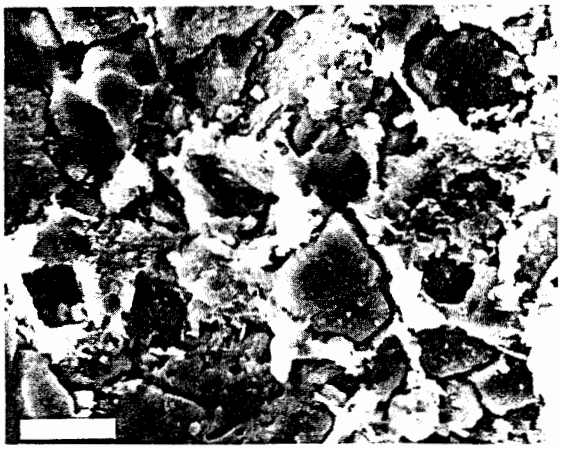

Fig. 7. Scanning electron microscopy photograph of silica cement in facies C3 limestone. Calcite crystals are *dark grey* and have smooth surfaces. Silica cement is *light gray* and has hackly surface. *Scale bar* is 10 μm long.

facies (Fig. 4E) have inclined baselines and positive Eu anomalies.

6. REE incorporation into carbonates

REE contents in ancient carbonate rocks were determined in a number of studies (e.g., Haskin et al., 1966; Jarvis et al., 1975), and it was found that REE concentrations are fairly low when compared to terrigenous rocks. In several studies (Haskin et al., 1966; Jarvis et al., 1975; Parekh et al., 1977; McLennan et al., 1979) it was documented that a rather high proportion of the REE's resides in the carbonate minerals. REE incorporation into carbonate minerals from seawater and diagenetic alteration of REE distribution was investigated by Parekh et al. (1977), Scherer and Seitz (1980), and Shaw and Wasserburg (1985). The latter authors found that primary marine carbonates contain only very small quantities of REE (e.g., $5 \cdot 10^{-5}$–$1.7 \cdot 10^{-2}$ ppm Sm), and that significant amounts of REE must have been added to ancient carbonate rocks (Haskin et al., 1966; Jarvis et al., 1975; Parekh et al., 1977; McLennan et al., 1979) during diagenesis in order to explain the observed discrepancies in

REE concentrations between modern and ancient carbonates.

7. REE in carbonates of the Newland Formation

As in other ancient carbonates, REE concentrations in carbonate rocks from the Newland Formation (Table III) are two to three orders of magnitude above those determined by Shaw and Wasserburg (1985) for modern carbonates. The question is, where the "excess" REE in the Newland carbonates came from and where they now reside. In addition, the variable baseline slopes of carbonate REE patterns and the positive Eu anomalies require explanation.

7.1. Relationship of REE *to clay fraction*

A general increase in REE's with Al_2O_3 in Fig. 8 suggests that a considerable portion of the "excess" REE's can be attributed to the terrigenous clastic fraction of the Newland carbonates. Illite is the main carrier of REE's in the Newland shales (Schieber, 1986), and it is thus reasonable to assume that the same is true for the associated carbonate rocks. Because the carbonate REE contents are normalized to an average of the shales that are interbedded with the carbonate units of the Newland Formation, and because the shales of the upper Newland Formation show considerable compositional uniformity (Schieber, 1985, 1986), one should expect any significant deviation of Newland carbonates from the REE distribution in the clay component (illite) of these rocks to be revealed by a departure from a flat REE pattern. For the 32 shale samples that were used for the UNAS composite, variability of REE content with respect to Al_2O_3 (Schieber, 1986) can be expressed by regression lines and associated standard deviations. For La for example, the regression line would be:

$$\text{La (ppm)} = 1.85 \times \text{Al}_2\text{O}_3\ (\%) + 8.3 \qquad (1)$$

with a standard deviation of ± 7.66 ppm, and for Lu it would be:

$$\text{Lu (ppm)} = 0.03 \times \text{Al}_2\text{O}_3\ (\%) + 0.078 \qquad (2)$$

with a standard deviation of ± 0.148 ppm. This variability has to be taken into account when we compare REE distribution in carbonate rocks with UNAS, and is shown as shale compositional trends in Fig. 8.

Fig. 8. shows that with regard to La and Al_2O_3, the data point scatter is considerably larger for limestone (Fig. 8B and D) than for dolostones (Fig. 8A), and that several limestone samples of facies C*3* plot even above the compositional trend of the shales (Fig. 8B). With regard to Lu and Al_2O_3 the data point scatter is much less pronounced, and all carbonate samples plot within the compositional trend of the shales (Fig. 8C).

Both, the flat baselines of the dolostone REE patterns (Fig. 4A and B) and Fig. 8A indicate that the REE content of the dolostones, with the exception of Eu, is most likely related to their clay component. Comparing the REE patterns of the various limestone facies (Fig. 4C, D and F) with the dolostones (Fig. 4A and B), the main difference appears to be that a considerable number of the limestones have inclined baselines, indicating a relative enrichment in light REE (LREE). LREE enrichment is strongest in facies C*3* which has the samples with the steepest baselines (Fig. 4C). Comparing La vs. Al_2O_3 relationships between dolostones and limestones (Fig. 8) shows, that whereas the dolostones follow the compositional trend of the shales, the data points for the limestones show considerably more scatter. If one uses strictly the compositional trend of the shales (eq. 1) as a criterion for La (and thus LREE) enrichment, 5 samples of facies C*3*, and one sample of facies C*4* show significant La (and LREE) enrichment. Because the dolostones have flat baselines and fall nicely into the compositional trends of the associated shales, one may even assume that they are closest in REE contents to the original clay com-

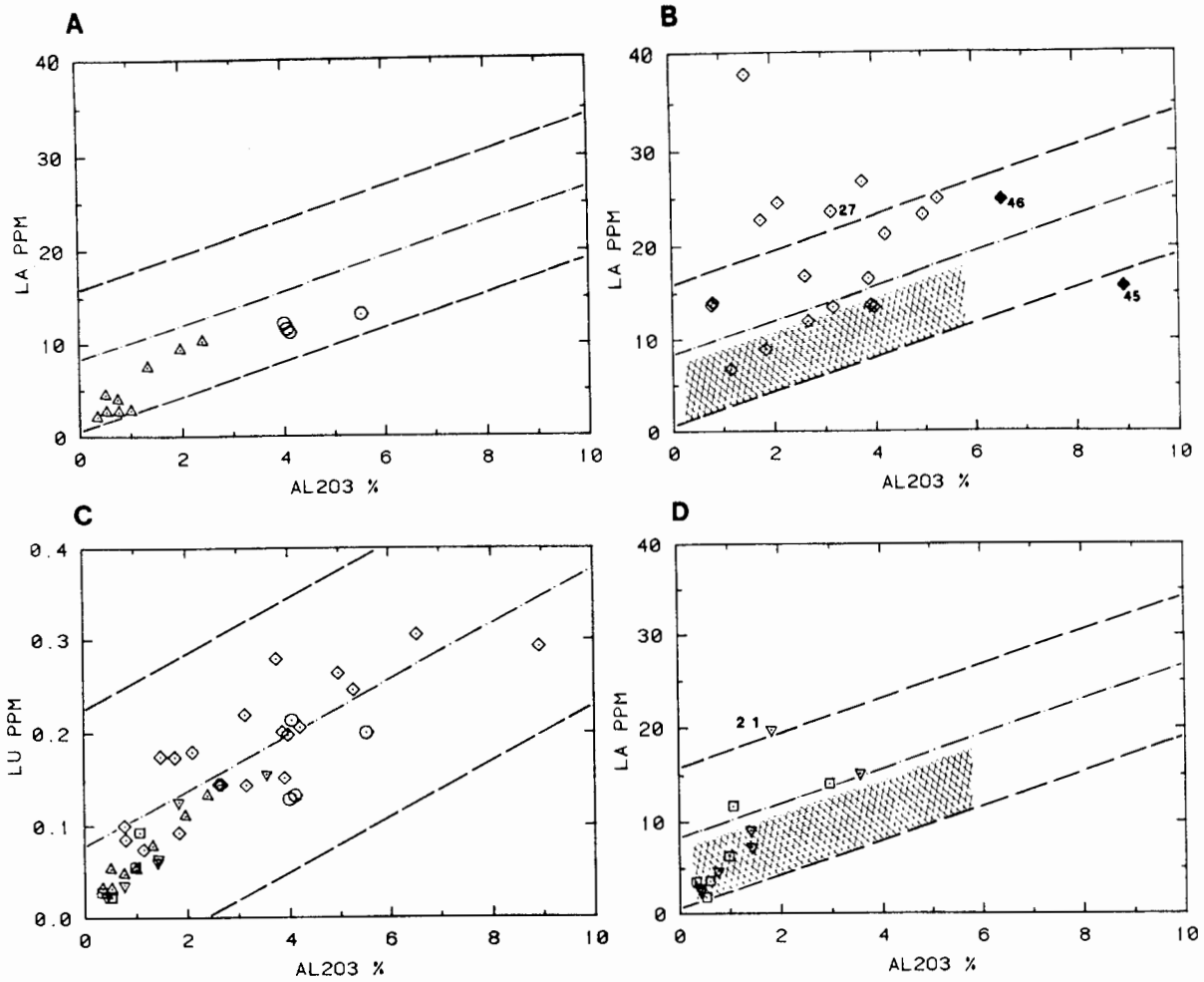

Fig. 8. Relationships between La, Lu and Al_2O_3 in the various facies types (similar plots with respect to Al_2O_3 can be produced for other REE's but are not shown here).
A. La vs. Al_2O_3 relationships for the dolostone samples (*circles* = facies C*1*; *triangles* = facies C2), the *dashed-dotted line* marks the position of compositional trend of shales (eq. 1), and the *dashed lines* mark the standard deviation for eq. 1;
B. La vs. Al_2O_3 for facies C*3* limestones (compositional trends of shales as in diagram (A). The *cross-lined area* indicates dolostone compositions, and the *solid black diamonds* mark samples of calcareous shale. The *numbers* refer to samples mentioned in the text;
C. Lu vs. Al_2O_3 relationships in Newland carbonates (*circles* = facies C*1*; *triangles* = facies C2; *diamonds* = facies C*3*; *inverse triangles* = facies C*4*, *squares* = facies C*6*). The *dashed-dotted line* represents eq. 2, and the *dashed lines* mark the standard deviation for eq. 2;
D. La vs. Al_2O_3 in facies C*4* (*inverse triangles*) and C*6* (*squares*). Compositional trends for shales as in diagram (A), *cross-lined area* indicates dolostone compositions.

ponent of the Newland carbonates, and that limestone samples that plot above the dolostone field in Fig. 8 are enriched in La (and LREE). Under this assumption even more limestone samples, 13 out of 18 samples of facies C*3*, 2 out of 7 samples of facies C*4*, and 2 out of 6 samples of facies C*6*, would be enriched in La (and LREE). Clearly, whichever way the matter is considered, the inclined baselines of the REE patterns, and the comparison of their La and Lu contents to associated shales and dolostones indicate variable degrees of LREE en-

richment in limestones, and further indicate that LREE enrichment is most common and significant in facies C3.

In summary one may say that the REE content of the majority of Newland carbonate samples is a consequence of their clay content. Relative to their associated shales most carbonate samples have positive Eu anomalies, the dolostones show no noticeable enrichment of either La or Lu, and the limestones, in particular facies C3, show variable degrees of La (or LREE) enrichment but essentially no enrichment of Lu (or HREE).

7.2. REE *partitioning*

Analyses of soluble and insoluble portions of four samples (Table II) show that between 85% and 96% of the La and between 47% and 86% of the Lu are contained in the soluble portion of these samples, and that the terrigenous fraction is impoverished in REE's when compared with REE concentrations in Newland shales, an indication of REE redistribution from clays to calcite. UNAS-normalized REE patterns of the carbonate–residue pairs (Fig. 9) show that the carbonate phase contains most of the REE in these samples, and that LREE are stronger enriched in the carbonate phase than HREE. Both, the carbonate phase and the residue show positive Eu anomalies. In addition, several analyses of carbonate fractions show Sm and Tb enrichment relative to the La–Lu baseline.

7.3. *Influence of diagenetic silica*

Samples of limestone facies C3 contain as much as 40% SiO_2, yet only a small portion of the silica can be traced to clay minerals and detrital quartz. Most of the silica exists as pore space fillings between calcite crystals. In samples with large silica contents interstitial silica forms a partial framework between calcite crystals, many of which are partialy or completely encased in diagenetic silica (Fig. 7). A plot of Al_2O_3/La ratios vs. SiO_2 for samples of facies C3 (Fig. 10) shows an increase of the Al_2O_3/La ratio with the SiO_2 content of the samples, an indication that diagenetic silica deposition had a negative influence on diagenetic La (and LREE) enrichment.

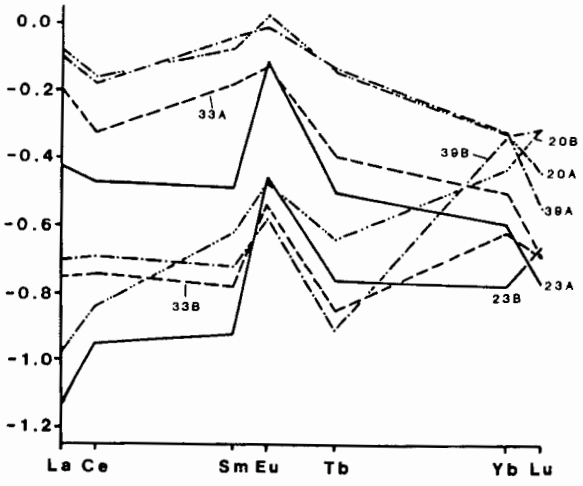

Fig. 9. REE patterns in carbonate-residue pairs (data in Table II). The *vertical axis* is the logarithm of the concentration ratio between sample and UNAS, and the *horizontal axis* is REE's by atomic number. The *numbers* to the right of REE patterns are sample numbers from Table II.

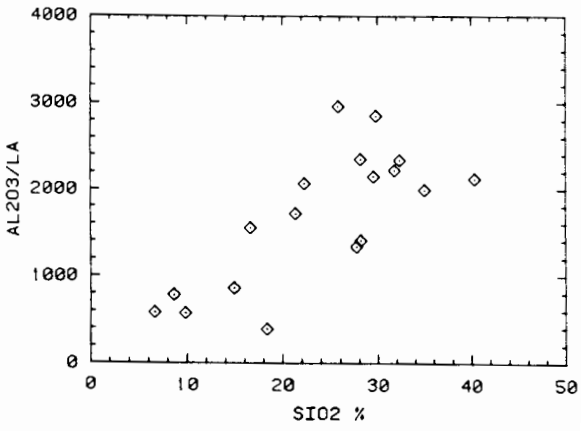

Fig. 10. Plot of Al_2O_3/La vs. SiO_2 for facies C3 indicating decreasing La enrichment (increasing Al_2O_3/La ratio) with increasing SiO_2 content.

8. Discussion

8.1. Relationship between facies, LREE *enrichment, and diagenesis*

Even though the REE's in the Newland carbonates appear to be mainly a consequence of the contained clay minerals, one notable feature is the enrichment of LREE's in the limestones relative to associated shales (Fig. 4). Also, LREE enrichment in facies C*3* is considerably larger than in facies C*4* and C*6* (Fig. 8). For a number of samples of facies C*3* the clay content is not large enough to explain the LREE contents of these samples (Fig. 8B), and an outside source is required. The calcareous shale interbeds in facies C*3* are one of the main distinctions between it and facies C*4* and C*6*, and it is suggested here that REE's are redistributed from shale interbeds to limestone beds during diagenesis. Facies C*3* resembles limestone–marl cycles that have been described elsewhere, and in which dissolution of $CaCO_3$ in shale–marl beds and reprecipitation of calcite in the growing limestone beds creates well-defined carbonate and shale beds during diagenesis (Eder, 1982; Ricken and Hemleben, 1982). The limestone beds in facies C*3* probably originated in the same way. Such a process requires extensive local mass transfer in aqueous solution between limestone and shale beds during diagenesis. This mass transfer is probably diffusion controlled in the case of concretionary carbonates (Berner, 1971). It is proposed that during diagenesis of facies C*3* not only calcite was redistributed, but REE's as well. Experiments by Haskin et al. (1966) showed that REE's are effectively removed from solution by calcite precipitation, and their results suggest that REE's are adsorbed on the surface of calcite crystals. Accordingly, calcite precipitation in the growing limestone beds of facies C*3* would have removed REE's from the surrounding pore waters and established a concentration gradient towards the limestone bed. The relatively high pH in calcite-saturated pore waters would tend to keep the REE content of the pore waters low, because under those pH conditions the bulk of the REE's would be precipitated as hydroxides (Haase et al., 1979). However, if by REE adsorption on calcite these pore waters are depleted in REE's below their supersaturation level with respect to REE-hydroxides, more REE can be released into solution from clay minerals. Thus, if calcite precipitation removes REE's from the pore waters (Haskin et al., 1966), then the REE concentration gradient and therefore REE redistribution from shale to limestone beds would continue as long as calcite precipitation in the limestone bed continues.

There are several lines of evidence to suggest that redistribution of REE (particularly of LREE) from shale interbeds to limestone beds did indeed occur in facies C*3*:

(1) The data from carbonate–residue pairs (Table II, Fig. 9) clearly show that at least *within* limestone beds REE's were redistributed from clay to calcite.

(2) The mere fact that a considerable number of limestone beds have LREE's in excess of what could be expected from their clay content indicates a net influx of REE's, and the shale interbeds are the closest available source.

(3) One sample of interlayer shale (sample *45*) was analyzed, and it shows a LREE content that is smaller than what should be expected from its clay content (Fig. 8B), and its REE pattern shows relative depletion of LREE (Fig. 11).

(4) The REE pattern of this shale sample is almost a mirror image (Fig. 11) of the pattern of the adjacent limestone bed (sample *27*) in terms of REE depletion and enrichment, another suggestion of REE redistribution between limestones and shale interbeds.

That REE redistribution is probably a local process whose effects are only noticeable in the immediate vicinity of a limestone bed is indicated by the fact that none of the shale units of the upper member of the Newland Formation show LREE depletion (Schieber, 1985, 1986),

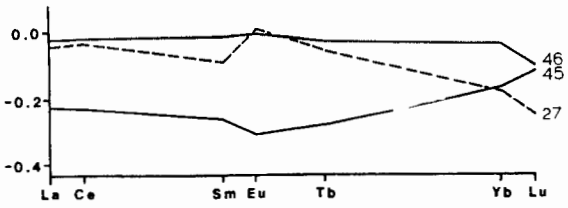

Fig. 11. REE distribution in a C3 limestone sample (No. 27), a directly adjacent bed of calcareous shale (No. 45), and a calcareous shale sample (No. 46) that was collected 1 m below the carbonate unit from which samples 27 and 46 were collected. *Vertical axis* is the logarithm of the concentration ratio between sample and UNAS, *horizontal axis* is REE's by atomic number.

and also by the REE pattern of sample *46* (Fig. 11). This sample was taken from a shale unit, just 1 m below the contact with an overlying carbonate unit that contained samples *27* and *45*. As can be seen in Fig. 11, sample *46* shows no sign of LREE depletion despite its proximity to the carbonate horizon. Thus, it appears that diagenetic REE redistribution from shale to limestone beds in facies C*3* was a local process and that its effects are not noticeable in adjacent shale packages.

Heavy REE's (HREE's) also experienced redistribution from clay to calcite within limestone beds, but to a lesser degree than is true for the LREE's (Table II). Considering the clay content of carbonate samples, no diagenetic addition of HREE's to carbonate beds can be demonstrated (Fig. 8C). It appears thus that all REE's are influenced by local redistribution, but that LREE's are much more strongly affected. This difference in behaviour between LREE's and HREE's can probably be related to the circumstance that LREE complexes are considerably less stable in solution (Goldberg et al., 1963; Haase et al., 1979; Cantrell and Byrne, 1987), and may therefore get adsorbed more readily onto calcite crystal surfaces (Haskin et al., 1966).

Facies C*4* and C*6* lack interbedded calcareous shales, and with the exception of sample *21* the samples show only minor diagenetic addition of LREE's (Fig. 8D). However, even though LREE contents can in all but one case be explained with the clay content of the samples, some degree of diagenetic LREE addition is indicated by the baseline slopes of the REE patterns (Fig. 4D and E). Sample *21*, which shows LREE enrichment comparable to facies C*3*, was taken from the top of a thin limestone horizon (1 m thick), and shales were thus directly adjacent to the forming limestone bed and could have supplied the excess REE's. However, such an explanation of LREE enrichment cannot be used for the other samples of facies C*4* and C*6*. Because interbedded shales can be excluded as a REE source during diagenesis, the only obvious source left are the pore waters that moved through the sediments during burial of the sequence. The much smaller magnitude of LREE enrichment in samples of facies C*4* and C*6* indicates that formation waters probably supplied REE's to the carbonates at a much smaller rate than did the local mass-transfer processes that were active during early diagenesis in facies C*3*.

8.2. Diagenetic silica deposition and LREE *enrichment*

Fig. 10 shows that diagenetic La enrichment in facies C*3* declines with an increase in diagenetic silica deposition. The intimate intergrowth of silica and calcite in these samples (Fig. 8) attests to more or less simultaneous calcite and silica deposition during early diagenesis. Thus one can plausibly argue that silica deposition between calcite crystals reduced porosity and limited diffusion of REE's into the carbonate beds. An additional effect of silica deposition would be to lower the total amount of calcite in a limestone bed, and because the calcite contains the bulk of the LREE's (Table III) the whole-rock LREE enrichment would be lower simply for that reason.

Facies C*4* and C*6* do not show any correlation between the Al_2O_3/La ratio and SiO_2 (plot not shown), even though diagenetic silica is found in these limestones as well. The difference may again be related to the lack of shale interbeds

in these facies. As noted above, these limestones probably experienced low-level REE addition from pore waters migrating along fractures and solution films of intercrystalline boundaries throughout burial history, but overall diagenetic LREE addition was much smaller than in facies C3 where probably a local redistribution process was operating during early diagenesis. In the case of facies C3 the bulk of LREE enrichment probably occurred during early diagenesis and therefore early-diagenetic silica precipitation had a strong influence on LREE enrichment. Later-diagenetic low-level REE addition may have occurred in facies C3, but is insignificant compared with the early-diagenetic component. In the case of facies C4 and C6 the early-diagenetic component of LREE addition is missing, and silica deposition was without noticeable effect because the bulk of LREE addition probably occurred later in diagenetic history.

Early-diagenetic silica deposition is pervasive in the dolostones of facies C1 and C2 and seems to have been able to shield these rocks quite effectively from any noticeable REE enrichment (except that of Eu) during diagenesis (Fig. 8A). One might of course also try to explain the lack of diagenetic REE addition with an inability of the dolomite crystal to accomodate these elements. However, a study of interlaminated limestones and dolostones by Kubanek and Parekh (1976) showed that dolomite was actually enriched in REE's relative to the coexisting calcite. Thus it appears that the lack of diagenetic REE enrichment (except that of Eu) in the dolostones was caused by early-diagenetic interstitial silica deposition, which prevented access of REE-bearing pore waters to the dolomite.

8.3. Positive Eu anomalies

Positive Au anomalies are common to the carbonates in this study and may be related to a positive Eu anomaly in the pore waters. In aqueous solution the REE's occur mainly as trivalent ions, usually complexed, and above a pH of 6 precipitation of REE-hydroxides occurs (Haase et al., 1979). Sm, Eu and Tb can also occur in the divalent state, and of the divalent REE Eu^{2+} is the most stable one in solution (Haase et al., 1979). The sediments of the Newland Formation are characterized by a common presence of organic matter, diagenetic pyrite and carbonate minerals. Shales in particular contain abundant pyrite and organic matter, and show evidence of dolomite recrystallization during diagenesis (Schieber, 1985). The association between organic matter and pyrite suggests that sulfate-reducing bacteria were the cause for pyrite formation. Baas Becking et al. (1960) measured Eh and pH conditions for sulfate reduction and iron sulfide formation in sediments, and found it to occur between pH 4.15 and 9.92 and down to Eh-values of -0.45 V. The oxidation potential from Eu^{2+} to Eu^{3+} is -0.43 V, and because the lower limit of water stability is a function of pH and Eh (Garrels and Christ, 1965), the minimum pH associated with such a small oxidation potential would have to be above 7.3. The presence of calcite and dolomite in the sediments of the Newland Formation indicates that the pH in the sediments was most likely above 8 (Baas Becking et al., 1960; Garrels and Christ, 1965), and thus the pH was probably large enough to allow reduction of Eu^{3+} to Eu^{2+}. The presence of abundant diagenetic pyrite and of organic matter throughout the Newland Formation (Schieber, 1985) attests to strongly reducing conditions in the sediments, and from above considerations it is quite possible that Eu existed as Eu^{2+} in the pore waters of the Newland Formation. Eu^{2+} probably existed as a soluble cation in these pore waters (Haase et al., 1979) because of its small ionic potential, and should have been more soluble than trivalent REE's whose concentrations were limited by precipitation of REE-hydroxides (because of relatively high pH of pore waters in carbonate sediments). It is thus quite possible that the pore waters of the Newland Formation were en-

riched in Eu and caused positive Eu anomalies in carbonates during diagenesis. The lack of positive Eu anomalies in six carbonate samples may indicate somewhat less reducing conditions in the sediment.

REE patterns of carbonate–residue pairs (Fig. 9) show that there was a net influx of Eu into the carbonate beds because both, the carbonate and the residue fraction show Eu enrichment. Thus the Eu must have been derived from the shales of the Newland Formation, and because it is likely that Eu travelled as the much more mobile Eu^{2+} ion, the shale units of the Newland Formation may have contributed Eu to pore waters fairly uniformly. Because the shales of the upper member of the Newland Formation have negative Eu anomalies (Schieber, 1986) when normalized to the North American Shale Composite (NASC), one might wonder if the Eu enrichment in the Newland carbonates is a potential cause for Eu depletion in the associated shales. A mass-balance calculation will show if this is indeed a reasonable assumption.

Eu enrichment in Newland carbonates was calculated as the difference between the measured value, and the Eu value derived from a straight-line interpolation between Sm and Tb, is given as ΔEu in Table III. The upper member of the Newland Formation in the Little Belt Mountains contains ~170 m of carbonate and ~360 m of shale. About 40 m of facies C2, ~60 m of facies C3, and ~70 m of facies C4 and C6 are present (facies C1 occurs only in the northernmost outcrops). An average ΔEu can be calculated for each facies, and the weighted average for the Newland carbonates as a whole calculates to $\Delta Eu = 0.074$ ppm. If we assume that this amount of excess Eu was derived from the shales, the Eu content of the average shale would have been lowered by just 0.035 ppm. The Eu deficit of the average shale of the upper member of the Newland Formation (UNAS) is 0.32 ppm (relative to NASC), ten times larger than the amount that was added to the Newland carbonates. Thus, it is obvious that negative Eu anomalies in Newland shales are related to the sediment source (Schieber, 1986), rather than to diagenetic Eu enrichment in Newland carbonates. Shale sample *45* (Fig. 11) indicates that Eu depletion of shales due to carbonate diagenesis will only be noticeable in the immediate vicinity of a carbonate bed.

Fig. 9 shows that besides Eu, there is also a certain degree of enrichment of the other intermediate REE's (IREE's), Sm and Tb, in the calcite of Newland carbonates. This minor enrichment may be due to replacement of Ca^{2+} ion by IREE because of similar ionic radii of Ca^{2+} and the IREE's (Goldberg et al., 1963).

9. Conclusions

The REE data from carbonates of the Proterozoic Newland Formation elucidate several influences of diagenetic processes on REE distribution in carbonate rocks. The main conclusions that can be drawn from this study are as follows:

(1) Significant local redistribution of REE, from shales to carbonates, occurs during the diagenetic growth of limestone beds and nodules.

(2) During this process there is a general tendency for LREE enrichment.

(3) Diagenetic REE addition to carbonate beds is reduced or inhibited by early-diagenetic interstitial silica deposition that prevents access of REE-bearing pore waters to carbonate beds.

(4) Positive Eu anomalies in these carbonate rocks probably indicate strongly reducing conditions during diagenesis.

(5) It is advantageous to normalize carbonate rocks to their associated unleached shales, because in this way the REE distribution in the carbonate phase can be more readily deciphered.

Acknowledgements

I would like to thank Drs. G.G. Goles, M.H. Reed, R. Cullers and J. Veizer for constructive

reviews of an earlier version of this manuscript. Field work in Montana and analytical work was supported by Anaconda Minerals Co.

References

Baas Becking, L.G.M., Kaplan, I.R. and Moore, D., 1960. Limits of the natural environment in terms of pH and oxidation-reduction potentials. J. Geol., 68: 243-284.

Balashov, Y.A., Ronov, A.B., Migdisov, A.A. and Turanskaya, N.V., 1964. The effect of climate and facies environment on the fractionation of rare earths during sedimentation. Geochem. Int., 2: 951-969.

Bathurst, R.C.G., 1983. Early diagenesis of carbonate sediments. In: A. Parker and B.W. Sellwood (Editors), Sediment Diagenesis. D. Reidel, Dordrecht, pp. 349-377.

Berner, R.A., 1971. Principles of Chemical Sedimentology. McGraw-Hill, New York, N.Y., 240 pp.

Cantrell, K.J. and Byrne, R.H., 1987. Rare earth element complexation by carbonate and oxalate ions. Geochim. Cosmochim. Acta, 51: 597-605.

Eder, W., 1982. Diagenetic redistribution of carbonate, a process in forming limestone-marl alternations (Devonian and Carboniferous, Rheinisches Schiefergebirge, West Germany). In: G. Einsele and A. Seilacher (Editors), Cyclic and Event Stratification. Springer, New York, N.Y., pp. 98-112.

Garrels, R.M. and Christ, C.L., 1965. Solutions, Minerals, and Equilibria. Harper & Row, New York, N.Y., 450 pp.

Goldberg, E.D., Koide, M., Schmitt, R.A. and Smith, R.H., 1963. Rare earth distributions in the marine environment. J. Geophys. Res., 68: 4209-4217.

Gordon, G.E., Rundle, K., Goles, G.G., Corliss, J.B., Benson, M.H. and Oxley, S.S., 1968. Instrumental activation analysis of standard rocks with high resolution gamma ray detectors. Geochim. Cosmochim. Acta, 32: 369-396.

Govindaraju, D., 1984. 1984 compilation of working values and sample description for 170 international reference samples of mainly silicate rocks and minerals. Geostand. Newsl., Spec. Iss., July 1984, 8: 3-16.

Haase, V., Kugler, H.K., Lehl-Thalinger, M. and Trobisch-Raussendorf, U., 1979. Sc, Y, La-Lu, Seltenerdelemente. In: M. Becke-Goehring (Editor), Gmelins Handbuch der anorganischen Chemie, Teil B7. Springer, Heidelberg, pp. 18-19.

Harrison, J.E., 1972. Precambrian Belt basin of northwestern United States: Its geometry, sedimentation, and copper occurrences. Geol. Soc. Am. Bull., 83: 1215-1240.

Hsakin, L.A., Wildeman, T.R., Frey, F.A., Collins, K.A., Keedy, C.R. and Haskin, M.A., 1966. Rare earths in sediments. J. Geophys. Res., 71: 6091-6105.

Haskin, L.A., Haskin, M.A., Frey, F.A. and Wildeman, T.R., 1968. Relative and absolute terrestrial abundances of the rare earths. In: L.H. Ahrens (Editor), Origin and Distribution of the Elements. Pergamon, Oxford, pp. 889-912.

Jarvis, J.C., Wildeman, T.R. and Banks, N.G., 1975. Rare earths in the Leadville Limestone and its marble derivates. Chem. Geol., 16: 27-37.

Kubanek, F. and Parekh, P.P., 1976. A study of the trace element distribution in an interlaminated limestone-dolostone. Geol. Jahrb., D-20: 23-39.

McLennan, S.M., Fryer, B.J. and Young, G.M., 1979. The geochemistry of the carbonate-rich Espanola Formation (Huronian) with emphasis on the rare earth elements. Can. J. Earth Sci., 16: 230-239.

Nelson, W.H., 1963. Geology of the Duck Creek Pass quadrangle, Montana. U.S. Geol. Surv., Bull. No. 1121J, 56 pp.

Parekh, P.P., Möller, P., Dulski, P. and Bausch, W.M., 1977. Distribution of trace elements between carbonate and non-carbonate phases of limestone. Earth Planet. Sci. Lett., 34: 39-50.

Piper, D.Z., 1974. Rare earth elements in the sedimentary cycle: A summary. Chem. Geol., 14: 285-304.

Ricken, W. and Hemleben, C., 1982. Origin of marl-limestone alternation (Oxford 2) in southwest Germany. In: G. Einsele and A. Seilacher (Editors), Cyclic and Event Stratification. Springer, New York, N.Y., pp. 63-71.

Ronov, A.B., Balashov, Y.A., Girin, Y.P., Bratishev, R.K. and Kazakov, G.A., 1974. Regularities of rare earth element distribution in the sedimentary shell and in the crust of the earth. Sedimentology, 21: 171-193.

Scherer, M. and Seitz, H., 1980. Rare earth element distribution in Holocene and Pleistocene corals and their redistribution during diagenesis. Chem. Geol., 28: 279-289.

Schieber, J., 1985. The relationship between basin evolution and genesis of stratiform sulfide horizons in Mid-Proterozoic sediments of Central Montana (Belt Supergroup). Ph.D. Dissertation, University of Oregon, Eugene, Oreg., 810 pp.

Schieber, J., 1986. Stratigraphic control of rare-earth pattern types in Mid-Proterozoic sediments of the Belt Supergroup, Montana, U.S.A.: Implications for basin analysis. Chem. Geol., 54: 135-148.

Shaw, H.F. and Wasserburg, G.J., 1985. Sm-Nd in marine carbonates and phosphates: Implications for Nd isotopes in seawater and crustal ages. Geochim. Cosmochim. Acta, 49: 503-518.